FIG. 3. Differential delay of 30- and 90-MHz sound waves versus round-trip path length (circles). Solid line, result expected for the prediction of Molinari and Regge (Ref. 3); dashed line, result according to the measurements of Anderson and Sabisky (Ref. 9).

see nothing approaching the expected magnitude for α_1. At the frequencies of our experiment any reasonable value for α_2 would lead to an effect that is completely unobservable within our resolution. The advantage of this experiment is that the only variable is the path length; as long as the amplitude of the reflected sound signal remains constant as the reflector is moved, then such undesirable effects as attenuation in the liquid, beam spreading, or tilting of the reflector must be absent. The very small amount of delay that we do occasionally observe does not tend to be reproducible or proportional to path length and is usually associated with some such amplitude effect.

The large amount of dispersion found by Anderson and Sabisky[9] is almost certainly due to the relatively high temperature at which they performed their experiment. At their temperature of 1.38 K the velocity can differ from its zero-temperature value by about 1%. It is not surprising, therefore, that the difference in the temperature dependence of the velocity for the different frequencies used by Anderson and Sabisky could account for the effect they observed.

The present experiment thus establishes that the magnitude of the coefficient of a quadratic term in the energy spectrum of ^{4}He must be less than 0.01 Å.

*Based on work performed under the auspices of the U. S. Atomic Energy Commission.

[1]N. E. Phillips, C. G. Waterfield, and J. K. Hoffer, Phys. Rev. Lett. 25, 1260 (1970).

[2]G. Barucchi, G. Ponzano, and T. Regge, to be published.

[3]A. Molinari and T. Regge, Phys. Rev. Lett. 26, 1531 (1971). We have adopted the sign convention of Eq. (2) of this reference.

[4]R. A. Cowley and A. D. B. Woods, Can. J. Phys. 49, 177 (1971).

[5]P. R. Roach, J. B. Ketterson, and M. Kuchnir, Phys. Rev. Lett. 25, 1002 (1970), also Phys. Rev. A 5, 2205 (1972).

[6]J. Jäckle and K. W. Kehr, Phys. Rev. Lett. 27, 654 (1971).

[7]H. J. Maris, Phys. Rev. Lett. 28, 277 (1972).

[8]P. R. Roach, J. B. Ketterson, B. M. Abraham, and M. Kuchnir, to be published, also unpublished.

[9]C. H. Anderson and E. S. Sabisky, Phys. Rev. Lett. 28, 80 (1972).

[10]Model 8708A; Hewlett-Packard Co., Mountain View, Calif. 94040.

Ion Heating via Turbulent Ion Acoustic Waves*

R. J. Taylor† and F. V. Coroniti

Department of Physics, University of California, Los Angeles, California 90024

Three-dimensional ion acoustic turbulence is excited by injecting a cold ion beam into a nonmagnetized plasma with $T_e/T_i > 5$. A rapid, approximately exponential heating of the ion beam is observed along the beam path. The heating rates level off when the ion temperature approaches $0.2T_e$. The turbulent ion acoustic wave energy density does not exceed $(1-3) \times 10^{-3} T_e$. Wave saturation, which occurs before significant dissipation of ion beam energy, is consistent with orbit-diffusion strong-turbulence theory.

Ion heating from electron-current–driven ion acoustic turbulence has been investigated in both linear and toroidal devices.[1-3] The turbulent-

heating experiment reported here differs from previous experiments in that there is no magnetic field and the ion acoustic turbulence is excited by

the ion-ion beam instability.[4-7] The two-ion-beam instability is currently thought to be responsible for the turbulent ion momentum loss and ion heating observed in high−Mach−number magnetosonic shocks and in low−Mach−number ion acoustic electrostatic shocks.[8,9] In analogy with electron-ion anomalous resistance, two-ion-beam driven turbulence produces an anomalous ion viscosity or an effective ion collision frequency.

The experiments are conducted in a double plasma device previously used for investigating electrostatic collisionless shocks.[10,11] The plasma dimensions are length = diam = 50 cm ∼ 1000 Debye lengths (λ_D), plasma density $n_p \sim 10^9$ cm^{-3}, ion temperature $T_i \sim 0.2$ eV (unheated), and variable electron temperature $T_e \sim 0.6–3.0$ eV. The ion beam is formed by accelerating source ions from one half of the device into a target plasma in the other half; electron flow at the interface is blocked by an electrostatic barrier imposed by a grid. Beam densities range from $n_b \sim 10^7$ to 10^9 cm^{-3} and typical beam velocities are $v_b \sim (2–4)c_s$ [$c_s = (T_e/M_i)^{1/2}$, the ion acoustic speed]. The acceleration of source ions through a potential φ_0 in the beam x direction decreases the parallel beam *temperature* $T_\parallel$ by a factor $q\varphi_0/T_i$ from the source temperature T_i, although the ion *energy spread* (as measured by an electrostatic energy analyzer[12]) remains insensitive to φ_0. Since the transverse beam temperature $T_\perp$ is unaffected, the beam is thermally anisotropic by a factor $T_\perp/T_\parallel \approx 20–50$. For $v_b > 2c_s$, the linear theory[4] of the ion-ion instability predicts that only ion acoustic modes with propagation vectors $\vec{k}$ oblique to the beam direction are unstable. The beam thermal anisotropy reduces the linear growth rate of waves near 90°.

The spatial evolution (steady-state conditions) of the parallel ion beam energy (right peak) is shown in Fig. 1(a) for $T_e/T_i < 5$, the linearly stable regime.[4] The beam is slightly attenuated because of charge-exchange collisions with background neutrals (mean free path $\approx 300\lambda_D$); no unstable waves are observed. Figure 1(b) shows the spatial evolution of the ion energy for $T_e = 3$ eV ($T_e/T_i \approx 15$) with all other parameters unchanged. The ion beam now slows down and is heated, eventually forming a quasilinear-type plateau near $x = 14$ cm ($300\lambda_D$); turbulent ion acoustic waves are measured by a spectrum analyzer.

Since the unstable waves have electric field components both parallel and transverse to the beam direction, the ion velocity distribution per-
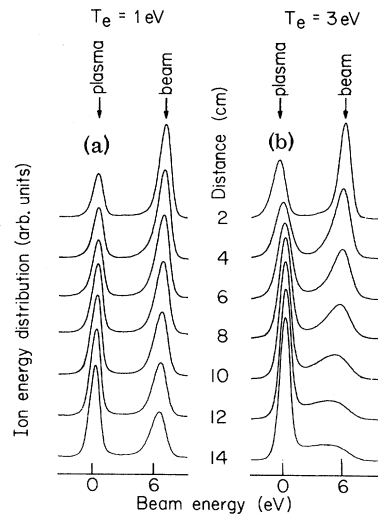

FIG. 1. Ion beam energy distribution for $n_b/n_p = 0.3$ as a function of beam penetration distance when the system is (a) stable and (b) unstable to ion acoustic waves. The variation of the height of the plasma peak at short distances is experimental.

pendicular to the beam is also heated by the turbulent electric fields.[5] Perpendicular ion heating is observed, but quantitative measurements are difficult since discrimination between the beam and background ion perpendicular velocity distributions, which initially have the same temperature, is required.

The beam-energy−analyzer data have been fitted by an approximate Maxwellian velocity distribution, thus yielding an effective temperature parameter $T_\parallel$. The spatial evolution of $T_\parallel$ for various beam-density and velocity v_b/c_s conditions is shown in Fig. 2(a). Only data for $v_b > 2c_s$ are shown, since, when $v_b < 2c_s$, the ion beam rapidly departs from a Maxwellian and forms a quasilinear-type plateau. The initial spatial increase of $T_\parallel$ is approximately exponential with growth length comparable to the linear instability growth length. The beam heating rate levels off when $T_\parallel \approx 0.2T_e$.

The spatial evolution of the ion acoustic turbulent wave spectrum is shown in Fig. 2(b) for $n_b/n_p = 0.1$ and 0.5. The spectrum is detected on a Langmuir probe with an approximately 45° directivity pattern, so that an accurate angular resolution of the wave spectrum was not possible. However, the wave energy did maximize at angles oblique to the beam direction. For $n_b/n_p = 0.1$ (top graph) the spectrum is dominated by frequencies $\omega \approx 0.6\omega_{pi}$ [$\omega_{pi} = (4\pi n q^2/M_i)^{1/2}$, the ion plasma frequency]. This region of the spectrum grows
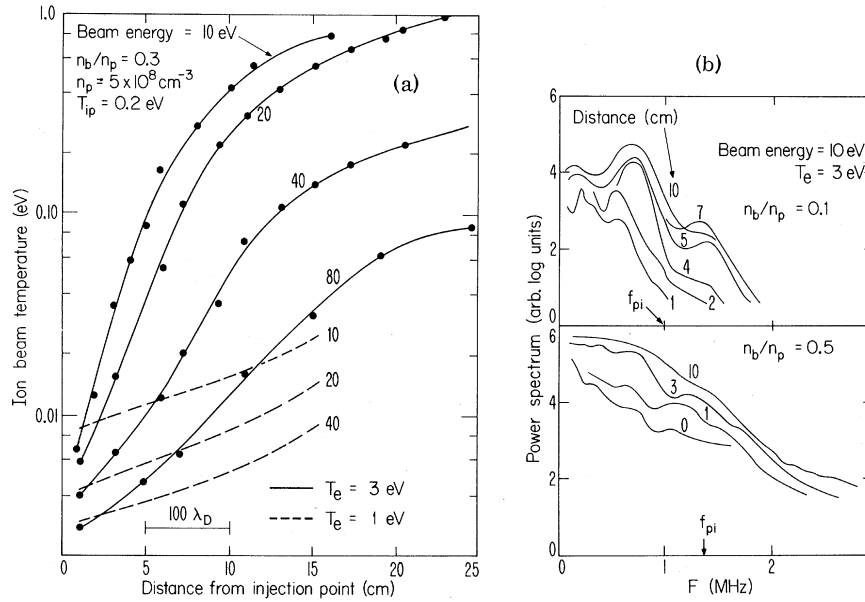
FIG. 2. (a) Turbulent heating of the ion beam as a function of beam penetration distance for beam velocities varying from $2c_s$ to $7c_s$. When $T_e = 3$ eV, the beam is unstable to ion acoustic waves. (b) Spectrum of ion acoustic waves for beam densities $n_b/n_p = 0.1$ and 0.5. Saturation wave energy density is $(1-3) \times 10^{-3} T_e$ for $n_b/n_p = 0.1$ and roughly a factor 2 greater for $n_b/n_p = 0.5$.

rapidly until around 4 cm ($80\lambda_D$) into the target plasma, at which point the growth rate is greatly reduced. The spectrum shape agrees with the fastest growing linear modes. For $n_b/n_p = 0.5$ (bottom graph) all frequencies in the spectrum reach saturation or have reduced growth rates at 6 cm; the spectrum has a monotonically decreasing shape with ω at all spatial locations. The spectrum shape is not governed by the fastest growing linear mode with $\omega \approx \omega_{pi}$, presumably because of nonlinear saturation. In both cases the growth-rate reduction or wave saturation occurs before the beam energy distribution undergoes significant distortion and well before the quasilinear-type plateau is formed. The saturated wave energy density $(\delta n/n_p)^2 = (q\, \delta\varphi/T_e)^2$, where $n(\delta\varphi)$ is the rms density (potential) fluctuation, does not exceed $(1-3) \times 10^{-3}$ for $n_b/n_p = 0.1$, and is about a factor of 2 higher for $n_b/n_p = 0.5$. Comparable saturated energy densities are measured in all ion-beam experiments regardless of whether the instability is a nonresonant beam type or a resonant inverse Landau instability of a low-density beam with v_b just above c_s.

Test waves at various ion acoustic frequencies have been propagated in all directions in the beam plasma after the beam turbulence has saturated. The top portion of Fig. 3 shows the pulse propa-

gation in an x-t plot when there is no beam, and only the principal ion acoustic mode is excited; the arrival time is $t = x/c_s$. The pulse suffers slight attenuation and dispersion as it propagates. When the beam is present (bottom portion of Fig. 3) both the slow ion acoustic and fast beam roots, arriving at $t = x/(c_x + v_b)$, are excited. The presence of the beam turbulence is evidenced by the trace broadening. The slow mode, which is unstable to the beam, initially grows rapidly, saturates, and then damps; the region of rapid growth is not shown in Fig. 3. The fast mode, which is unstable, just damps spatially. Regardless of the propagation direction, all test waves were observed to damp much faster than the total turbulent wave energy, which remained roughly constant. Therefore turbulent wave saturation must be interpreted as a steady-state balance between unstable wave growth and nonlinear damping processes.

The low rms wave amplitudes suggest that conventional mode-coupling and nonlinear Landau damping processes are not dominant (calculations substantiate this point). Furthermore, since growth-rate reduction or wave saturation occurs prior to a significant relaxation of the beam distribution function, quasilinear plateau formation is not responsible for saturation. Recent plasma turbulence theories[12,13] have emphasized that
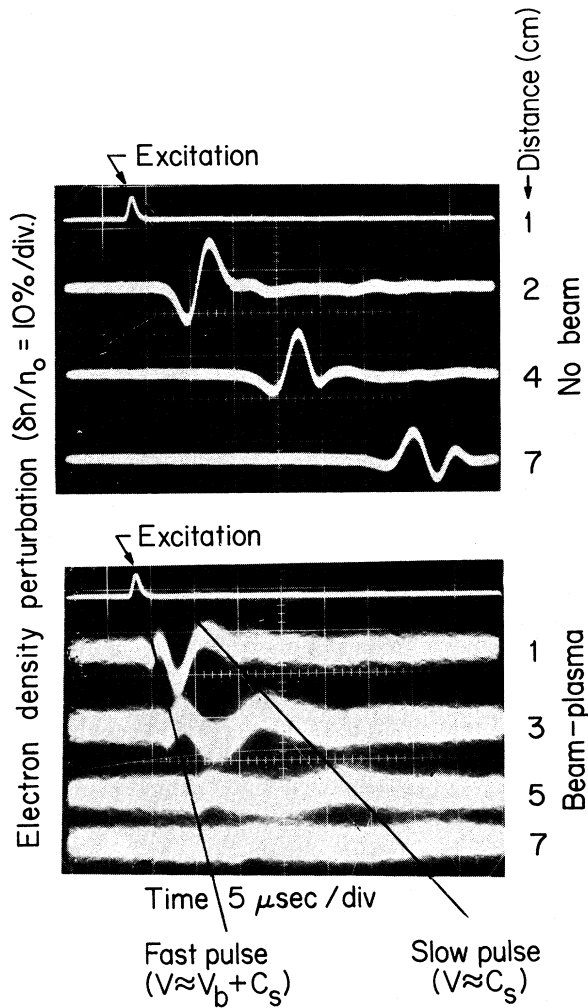
tion[12,13] for the real part ω_R and imaginary part γ_k of the wave frequency is

$$\omega_R = \vec{k} \cdot \vec{v}_b - n^{1/3} k c_s / 4^{2/3} (1 + k^2 \lambda_D^2)^{1/2},$$

$$\gamma_k = - \nu_{eff} + \sqrt{3}\, n^{1/3} k c_s / 4^{2/3} (1 + k^2 \lambda_D^2)^{1/2}. \tag{1}$$

Wave saturation $\gamma_k = 0$ occurs when ν_{eff} becomes comparable to the initial linear growth rate (term proportional to $n^{1/3}$). $\nu_{eff}(\vec{v}_b)$ can be determined in terms of the potential fluctuations φ_k from the diffusion tensor[12,13] with $\gamma_k = 0$. For the relatively narrow spectrum of the beam turbulence when $n \ll 1$, we find

$$\nu_{eff}(\vec{v}_b) \approx k_* c_s [\textstyle\sum_k q^2 |\varphi_k^2| / T_e^2]^{1/4}, \tag{2}$$

where k_* is a typical wave number and q is the electronic charge. Combining (1) and (2) we have

$$\sum_k \frac{q^2 |\varphi_k^2|}{T_e^2} \approx \frac{9}{4^{8/3}} \frac{n^{4/3}}{(1 + k_*^2 \lambda_D^2)^2} \qquad \bullet \tag{3}$$

which for $n \sim 0.1$, $k \lambda_D \sim 1$, yields $\sum_k q^2 |\varphi_k^2| / T_e^2 \approx 3 \times 10^{-3}$, in rough agreement with experimental saturation levels. Equation (3) actually overestimates the wave energy density since the growth rate is reduced by diffusion from its initial linear value. The beam energy decay length L_b can be estimated from the v_x moment of the beam diffusion equation,[12,13]

$$\frac{\partial}{\partial x} \left(\frac{n_b M_+ v_b^2}{2} \right)$$

$$\equiv \frac{n_b M_+ v_b^2}{2 L_b} = -2 \sum_k \frac{q^2 |\varphi_k|^2 k^2 k_x}{M_+ \nu_{eff}^3 (\vec{v}_b)} n_b (\vec{k} \cdot \vec{v}_b - \omega_k). \tag{4}$$

Substitution of (1), (2), and (3) into (4) yields $L_b \sim (10^2 - 2 \times 10^2) \lambda_D$, in rough agreement with experimental values (Figs. 1 and 2).

At wave saturation the ion beam still has considerable free energy available for wave growth. The observed initial growth, saturation, and damping of test waves in a turbulent beam-plasma and the above theory imply that wave saturation is a dynamic balance between the emission of waves by the beam and the destruction or damping of wave coherence by the turbulent diffusion of particle orbits. The beam continues to lose directed energy and heat until diffusion sufficiently broadens the beam distribution function so that wave emission ceases. In numerical simulation experiments, Forslund and Shonk[5] showed that two equal ion beams heated until $T_e / T_b \approx 3.5$ was reached, at which point the ion acoustic waves were linearly stable. The final ion beam temperature $T_b \approx 0.2 T_e$ observed in our

FIG. 3. Test-wave propagation in a plasma without a beam (top) and with an $n_b/n_p = 0.3$ beam (bottom). In the presence of beam-driven ion acoustic turbulence both the slow and fast modes damp much faster than the turbulent wave energy.

wave stabilization may result from the diffusion of particle orbits arising from the turbulent wave fields. Since the experimental turbulent wave spectrum is three-dimensional, the strong-turbulence wave-particle correlation should be a statistical trapping rather than the complete trapping possible for one-dimensional, narrow-bandwidth waves. In essence, a wave-particle correlation exists for only an effective collision time ν_{eff}^{-1} $\{\nu_{eff}(\vec{v}) = [\vec{k} \cdot \vec{D}(\vec{v}) \cdot \vec{k}]^{1/3}$, where $\vec{D}(\vec{v})$ is the diffusion tensor} before being destroyed by the other random fluctuations.

For simplicity, we consider only a weak beam $n = n_b/n_p \ll 1$, $T_e/T_i \gg 1$, and $v_b > 2 c_s$. The approximate solution of the nonlinear dielectric func-

experiments roughly agrees with their results.

It is a pleasure to acknowledge many illuminating discussions with Professor K. MacKenzie, Professor C. F. Kennel, and Professor B. D. Fried and with Dr. H. Ikezi and Dr. P. Barrett.

---

[1]T. Kawabe, J. Iannucci, and H. Eubank, Phys. Rev. Lett. 25, 642 (1971); A. Hirose, I. Alexeff, W. D. Jones, S. T. Uch, and K. E. Lonngren, Phys. Rev. Lett. 25, 1563 (1970).

[2]S. Q. Mak, H. Skarsgard, and A. R. Strilchuk, Phys. Rev. Lett. 25, 1409 (1970). This paper contains extensive references to previous work.

[3]T. Jensen and F. R. Scott, Phys. Fluids 11, 1809 (1968).

[4]B. D. Fried and A. Y. Wong, Phys. Fluids 9, 1084 (1966).

[5]D. W. Forslund and C. R. Shonk, Phys. Rev. Lett. 24, 579 (1970).

[6]R. C. Davidson, N. A. Krall, K. Papadopoulos, and R. Shanny, Phys. Rev. Lett. 24, 579 (1970).

[7]A. G. Borisenko and G. S. Kirichenko, Zh. Eksp. Teor. Fiz. 60, 384 (1970) [Sov. Phys. JETP 33, 207 (1971)].

[8]R. J. Taylor, D. R. Baker, and H. Ikezi, Phys. Rev. Lett. 24, 206 (1970).

[9]A. Y. Wong and R. W. Means, Phys. Rev. Lett. 27, 973 (1971).

[10]A description of the energy analyzer used is given in H. Ikezi and R. J. Taylor, J. Appl. Phys. 41, 738 (1970).

[11]I. Alexeff, W. D. Jones, and K. E. Lonngren, Phys. Rev. Lett. 21, 878 (1968); L. S. Hall and W. Heckrotte, Phys. Rev. 166, 120 (1968).

[12]T. H. Dupree, Phys. Fluids 9, 1773 (1966).

[13]J. Weinstock, Phys. Fluids 12, 1045 (1969).

Torque on a Rayleigh Disk Due to He II Flow*

Walter J. Trela

Department of Physics, Haverford College, Haverford, Pennsylvania 19041

(Received 30 March 1972)

A model for He II flow past a Rayleigh disk is presented which assumes that superfluid potential flow and normal fluid Helmholtz flow occur. A torque which increases as the temperature decreases is predicted, agreeing with Pellam's measurements in rotating helium below T_λ. New measurements of the torque on a Rayleigh disk in nonrotating helium are presented, indicating Helmholtz flow above T_λ, a continuous torque at the λ point, and increasing torque below T_λ.

The Rayleigh disk has been used in several experiments[1-7] to probe the local velocity field of He II. However, the flow pattern around the disk is still not well understood.[8] Particularly puzzling are Pellam's experimental results[1-4] in rotating He II, which indicate a decreasing torque as the temperature is increased toward the λ point.

We present here a simple model for the flow of He II past a Rayleigh disk, which predicts a temperature-dependent torque below T_λ as observed by Pellam. New experimental results are also presented in nonrotating He II, which are in at least qualitative agreement with this model.

The classical flow pattern for a perfect (nonviscous) liquid around a Rayleigh disk is potential flow. The superfluid component of He II provides the only real liquid capable of perfect potential flow, and experiments[7,9] indicate that at sufficiently low velocity, potential flow does take place. A flat rectangular disk (width w and height d) exposed to pure potential flow will experience a torque of the form[10]

$$\tau = \tfrac{1}{8}\pi w^2 d\rho v^2 \sin 2\theta, \qquad (1)$$

where ρ is the fluid density, v the undisturbed fluid velocity, and θ the angle between the disk and fluid velocity.

Normal viscous liquids *do not* move past a Rayleigh disk with potential flow. Instead, flow separation with a velocity discontinuity occurs at the disk edges and a stagnant region exists behind the disk.[11] By direct observation, Kitchens *et al.*[12] have seen velocity fields of this general
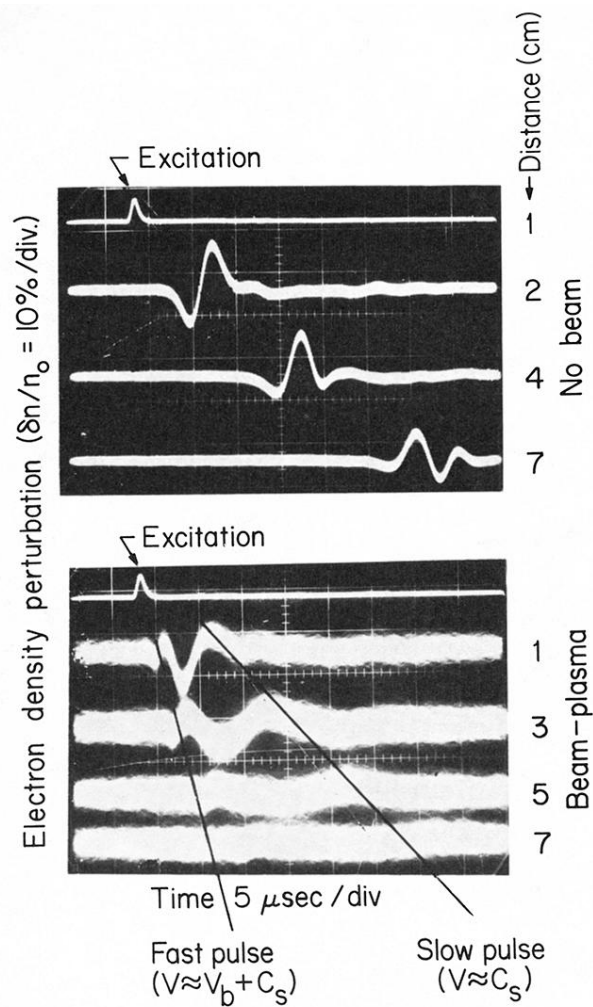
FIG. 3. Test-wave propagation in a plasma without a beam (top) and with an $n_b/n_p = 0.3$ beam (bottom). In the presence of beam-driven ion acoustic turbulence both the slow and fast modes damp much faster than the turbulent wave energy.